J Sci Comput (2009) 40: 375–390
DOI 10.1007/s10915-008-9262-0

Local Discontinuous Galerkin Method for Surface Diffusion and Willmore Flow of Graphs

Yan Xu · Chi-Wang Shu

Received: 17 May 2008 / Revised: 26 September 2008 / Accepted: 8 December 2008 /
Published online: 18 December 2008

Abstract In this paper, we develop a local discontinuous Galerkin (LDG) finite element method for surface diffusion and Willmore flow of graphs. We prove L^2 stability for the equation of surface diffusion of graphs and energy stability for the equation of Willmore flow of graphs. We provide numerical simulation results for different types of solutions of these two types of the equations to illustrate the accuracy and capability of the LDG method.

Keywords Local discontinuous Galerkin method · Surface diffusion of graphs · Willmore flow of graphs · Stability

1 Introduction

In this paper, we consider the surface diffusion of graphs

$$u_t + \nabla \cdot \left(Q \left(\boldsymbol{I} - \frac{\nabla u \otimes \nabla u}{Q^2} \right) \nabla H \right) = 0 \tag{1.1}$$

Y. Xu research supported by NSFC grant 10601055 and Foundation for Authors of Excellent Doctoral Dissertations of the Chinese Academy of Sciences.
C.-W. Shu research supported in part by NSFC grant 10671190 during his visit to the Department of Mathematics, University of Science and Technology of China, Hefei, Anhui 230026, P.R. China. Additional support is provided by NSF grants DMS-0510345 and DMS-0809086 and by DOE grant DE-FG02-08ER25863.

Y. Xu (✉)
Department of Mathematics, University of Science and Technology of China, Hefei, Anhui 230026, People's Republic of China
e-mail: yxu@ustc.edu.cn

C.-W. Shu
Division of Applied Mathematics, Brown University, Providence, RI 02912, USA
e-mail: shu@dam.brown.edu

and the equation of Willmore flow of graphs

$$u_t + Q\nabla\cdot\left(\frac{1}{Q}\left(\boldsymbol{I}-\frac{\nabla u\otimes\nabla u}{Q^2}\right)\nabla(QH)\right)-\frac{1}{2}Q\nabla\cdot\left(\frac{H^2}{Q}\nabla u\right)=0, \tag{1.2}$$

where Q is the area element

$$Q=\sqrt{1+|\nabla u|^2} \tag{1.3}$$

and H is the mean curvature of the domain boundary Γ

$$H=\nabla\cdot\left(\frac{\nabla u}{Q}\right). \tag{1.4}$$

There are many applications of these models, such as body shape dynamics, surface construction, computer data processing, image processing and so on. These two equations are both highly nonlinear fourth-order PDEs. They are different from second order geometric evolution problems, such as mean curvature motion, since no maximum principle is known [16] for fourth order problems. The higher order differential operators and additional nonlinearities for these kind of problems are difficult to analyze and to simulate numerically. In this paper we will construct stable high order accurate methods based on spatial discretizations by local discontinuous Galerkin finite element methods.

The surface diffusion equation [15]

$$V=\Delta_\Gamma H \quad \text{on } \Gamma \tag{1.5}$$

models the diffusion of mass within the bounding surface of a solid body, where V is the normal velocity of the evolving surface Γ,

$$V=-\frac{u_t}{Q(u)}, \tag{1.6}$$

and Δ_Γ denotes the Laplace-Beltrami operator

$$\Delta_\Gamma v=\frac{1}{Q(u)}\nabla\cdot\left(Q(u)\left(\boldsymbol{I}-\frac{\nabla u\otimes\nabla u}{Q(u)^2}\right)\nabla v\right). \tag{1.7}$$

Equation (1.5) is described as a mechanism of surface formation under the action of a chemical potential. For a surface with constant surface energy density, the appropriate chemical potential in this setting is the mean curvature H. The existence, uniqueness and regularity are discussed in [20, 21]. In [19], the authors describe an algorithm for the evolution of elastic curves. Some interesting computational results have been collected in [1, 3, 15, 19]. In [3], a finite difference scheme was discussed for the surface diffusion of graphs. A space-time finite element method for axially symmetric surfaces is presented by Coleman, Falk and Moakher in [12]. In [1], Bänsch, Morin and Nochetto presented a variational formulation for graphs and derived a priori error estimates for a semi-discrete finite element discretization. Deckelnick, Dziuk and Elliott provided an error analysis [15] for the anisotropic case.

A similar evolution law is the Willmore flow

$$V=\Delta_\Gamma H+\frac{1}{2}H^3-2HK, \tag{1.8}$$

where K is the Gauss curvature of Γ. The Willmore functional

$$\mathcal{W}_\Gamma = \int_\Gamma H^2 ds = \int_\Omega H^2 Q d\Omega \tag{1.9}$$

expresses the elastic energy of the surface. The Willmore flow is an evolutionary law for minimizing mean curvature of curves or surfaces. Issues about the boundary value problems for Willmore flow are not completely settled. We refer the reader to [24] and references therein. In [14], an implicit numerical scheme for the Willmore flow of graphs based on a finite element method together with its numerical analysis is presented. A level set formulation for the Willmore flow can be found in [16]. Asymptotical convergence of the phase-field model for the Willmore flow was proved and numerical simulations were performed by finite difference methods in [17, 18]. A finite difference scheme for the Willmore flow of graphs was discussed in [22].

In this paper we pay particular attention to the discontinuous finite element method, specifically, to the local discontinuous Galerkin (LDG) method. The considered LDG method is a particular version of the discontinuous Galerkin (DG) method, which uses a completely discontinuous piecewise polynomial space for the numerical solution and the test functions. It was first designed as a method for solving hyperbolic conservation laws containing only first order spatial derivatives, e.g. Reed and Hill [23] for solving linear equations, and Cockburn et al. [5, 6, 10, 11] for solving nonlinear hyperbolic equations.

Later, the LDG method was introduced by Cockburn and Shu in [7] as an extension of the Runge-Kutta DG (RKDG) method to general convection-diffusion problems, and of the DG scheme for the compressible Navier-Stokes equations proposed by Bassi and Rebay in [2]. More general information about DG methods for elliptic and hyperbolic partial differential equations can be found in [4, 8, 9, 13]. The idea of the LDG method is to rewrite the equations with higher order derivatives into a first order system, then apply the discontinuous Galerkin method on the system. The design of the numerical fluxes is the key ingredient to ensure stability.

Recently, the LDG techniques have been developed for various nonlinear wave equations with high order derivatives [27–29]. In [25, 26], the LDG methods with provable energy stability were designed for the Cahn-Hilliard equations and the Allen-Cahn/Cahn-Hilliard system which are also nonlinear fourth-order equations. In these papers, stable and high order accurate LDG methods for quite general nonlinear wave equations including multi-dimensional and system cases have been developed. The proof of the nonlinear L^2 stability of these methods was usually given and successful numerical experiments demonstrate their capability. These results indicate that the LDG method is a good tool for solving nonlinear equations in mathematical physics.

The DG method possesses several properties to make it very attractive for practical computations, such as easy parallelization, easy adaptivity, and simple treatment of boundary conditions. The most important property of this method is its strong stability and high-order accuracy. All of these good properties motivate us to develop the LDG method for curvature flow problems.

The paper is organized as follows. In Sect. 2, we present and analyze our LDG method for the surface diffusion of graphs equation (1.1). The details of the LDG method and the proof of L^2 stability are described. In Sect. 3, we present the LDG method for the Willmore flow of graphs equation (1.2). We give a proof of the energy stability in Sect. 3.2. Section 4 contains numerical results for nonlinear problems which include the surface diffusion of graphs and Willmore flow of graphs. These numerical results demonstrate the accuracy and capability of the LDG methods. Concluding remarks are given in Sect. 5.

2 The LDG Method for the Surface Diffusion of Graphs

In this section, we consider the local discontinuous Galerkin method for the surface diffusion of graphs equation (1.1) in $\Omega \in \mathbb{R}^d$ with $d \leq 3$. Although we do not address numerical results in three dimensions in this paper, the LDG methods and the stability results of this paper are valid for all $d \leq 3$.

2.1 Notation

Let $\mathcal{T}_h$ denote a tessellation of Ω with shape-regular elements K. Let Γ denote the union of the boundary faces of elements $K \in \mathcal{T}_h$, i.e. $\Gamma = \bigcup_{K\in\mathcal{T}_h} \partial K$, and $\Gamma_0 = \Gamma \backslash \partial\Omega$.

In order to describe the flux functions we need to introduce some notations. Let e be a face shared by the "left" and "right" elements K_L and K_R (we refer to [29] and [25] for a proper definition of "left" and "right" in our context). Define the normal vectors ν_L and ν_R on e pointing exterior to K_L and K_R, respectively. If ψ is a function on K_L and K_R, but possibly discontinuous across e, let ψ_L denote $(\psi|_{K_L})|_e$ and ψ_R denote $(\psi|_{K_R})|_e$, the left and right trace, respectively.

Let $\mathcal{P}^p(K)$ be the space of polynomials of degree at most $p \geq 0$ on $K \in \mathcal{T}_h$. The finite element spaces are denoted by

$$V_h = \left\{\varphi \in L^2(\Omega) : \varphi|_K \in \mathcal{P}^p(K),\ \forall K \in \mathcal{T}_h\right\},$$

$$\Sigma_h = \left\{\boldsymbol{\eta} = (\eta_1, \ldots, \eta_d)^T \in (L^2(\Omega))^d : \eta_l|_K \in \mathcal{P}^p(K), l = 1, \ldots, d,\ \forall K \in \mathcal{T}_h\right\}.$$

Note that functions in V_h and Σ_h are allowed to have discontinuities across element interfaces.

Here we only consider periodic boundary conditions. Notice that the assumption of periodic boundary conditions is for simplicity only and not essential: the method can be easily designed for non-periodic boundary conditions. The development of the LDG method for the non-periodic boundary conditions can be found in [25, 26].

2.2 The LDG Method

To define the local discontinuous Galerkin method, we rewrite (1.1) as a first order system:

$$u_t + \nabla \cdot \boldsymbol{s} = 0, \tag{2.1a}$$

$$\boldsymbol{s} - \boldsymbol{E}(\boldsymbol{r})\boldsymbol{p} = 0, \tag{2.1b}$$

$$\boldsymbol{p} - \nabla H = 0, \tag{2.1c}$$

$$H - \nabla \cdot \boldsymbol{q} = 0, \tag{2.1d}$$

$$\boldsymbol{q} - \frac{\boldsymbol{r}}{Q} = 0, \tag{2.1e}$$

$$\boldsymbol{r} - \nabla u = 0, \tag{2.1f}$$

with

$$\boldsymbol{E}(\boldsymbol{r}) = Q\left(\boldsymbol{I} - \frac{\boldsymbol{r}\otimes\boldsymbol{r}}{Q^2}\right), \tag{2.2}$$

$$Q = \sqrt{1 + |\boldsymbol{r}|^2}, \tag{2.3}$$

where $\boldsymbol{s}$, $\boldsymbol{p}$, $\boldsymbol{q}$, $\boldsymbol{r}$ are vectors, $\boldsymbol{E}(\boldsymbol{r})$ is the $d \times d$ matrix and $\boldsymbol{I}$ is the $d \times d$ identity matrix.

Applying the LDG method to the system (2.1), we have the scheme: Find $u, H \in V_h$, $\boldsymbol{s}$, $\boldsymbol{p}, \boldsymbol{q}, \boldsymbol{r} \in \Sigma_h$, such that, for all test functions $\varphi, \vartheta \in V_h$ and $\boldsymbol{\phi}, \boldsymbol{\eta}, \boldsymbol{\rho}, \boldsymbol{\zeta} \in \Sigma_h$, we have

$$\int_K u_t \varphi dK - \int_K \boldsymbol{s} \cdot \nabla \varphi dK + \int_{\partial K} \widehat{\boldsymbol{s} \cdot \boldsymbol{\nu}} \varphi ds = 0, \tag{2.4a}$$

$$\int_K \boldsymbol{s} \cdot \boldsymbol{\phi} dK - \int_K \boldsymbol{E}(\boldsymbol{r}) \boldsymbol{p} \cdot \boldsymbol{\phi} dK = 0, \tag{2.4b}$$

$$\int_K \boldsymbol{p} \cdot \boldsymbol{\eta} dK + \int_K H \nabla \cdot \boldsymbol{\eta} dK - \int_{\partial K} \widehat{H} \boldsymbol{\nu} \cdot \boldsymbol{\eta} ds = 0, \tag{2.4c}$$

$$\int_K H \vartheta dK + \int_K \boldsymbol{q} \cdot \nabla \vartheta dK - \int_{\partial K} \widehat{\boldsymbol{q} \cdot \boldsymbol{\nu}} \vartheta ds = 0, \tag{2.4d}$$

$$\int_K \boldsymbol{q} \cdot \boldsymbol{\rho} dK - \int_K \frac{\boldsymbol{r}}{Q} \cdot \boldsymbol{\rho} dK = 0, \tag{2.4e}$$

$$\int_K \boldsymbol{r} \cdot \boldsymbol{\zeta} dK + \int_K u \nabla \cdot \boldsymbol{\zeta} dK - \int_{\partial K} \widehat{u} \boldsymbol{\nu} \cdot \boldsymbol{\zeta} ds = 0, \tag{2.4f}$$

where $\boldsymbol{E}(\boldsymbol{r})$ and Q are computed by (2.2) and (2.3).

The "hat" terms in (2.4) at the cell boundary obtained after integration by parts are the so-called "numerical fluxes", which are functions defined on the cell edges and should be designed based on different guiding principles for different PDEs to ensure stability. It turns out that we can take the simple choices

$$\widehat{\boldsymbol{s}}|_e = \boldsymbol{s}_L, \qquad \widehat{\boldsymbol{q}}|_e = \boldsymbol{q}_R, \qquad \widehat{H}|_e = H_L, \qquad \widehat{u}|_e = u_R \tag{2.5}$$

which ensure L^2 stability.

2.3 L^2 Stability

In this section, we prove the L^2 stability of the LDG method for the surface diffusion of graphs defined in the previous section.

Proposition 2.1 (L^2 stability) *The solution of the surface diffusion of graphs using the schemes* (2.4)–(2.5) *satisfies* L^2 *stability*

$$\frac{1}{2} \frac{\mathrm{d}}{\mathrm{d}t} \int_\Omega u^2 d\Omega + \int_\Omega H^2 d\Omega = 0, \quad \forall u, H \in V_h. \tag{2.6}$$

Proof We take the test functions

$$\varphi = u, \qquad \boldsymbol{\phi} = \boldsymbol{r}, \qquad \boldsymbol{\eta} = \boldsymbol{q}, \qquad \vartheta = H, \qquad \boldsymbol{\rho} = -\boldsymbol{p}, \qquad \boldsymbol{\zeta} = -\boldsymbol{s}.$$

Then we have

$$\int_K u_t u dK - \int_K \boldsymbol{s} \cdot \nabla u dK + \int_{\partial K} \widehat{\boldsymbol{s} \cdot \boldsymbol{\nu}} u ds = 0, \tag{2.7a}$$

$$\int_K \boldsymbol{s} \cdot \boldsymbol{r} dK - \int_K \boldsymbol{E}(\boldsymbol{r}) \boldsymbol{p} \cdot \boldsymbol{r} dK = 0, \tag{2.7b}$$

$$\int_K \boldsymbol{p}\cdot\boldsymbol{q}dK + \int_K H\nabla\cdot\boldsymbol{q}dK - \int_{\partial K}\widehat{H}\boldsymbol{v}\cdot\boldsymbol{q}ds = 0, \tag{2.7c}$$

$$\int_K H^2 dK + \int_K \boldsymbol{q}\cdot\nabla H dK - \int_{\partial K}\widehat{\boldsymbol{q}\cdot\boldsymbol{v}}Hds = 0, \tag{2.7d}$$

$$-\int_K \boldsymbol{q}\cdot\boldsymbol{p}dK + \int_K \frac{\boldsymbol{r}}{Q}\cdot\boldsymbol{p}dK = 0, \tag{2.7e}$$

$$-\int_K \boldsymbol{r}\cdot\boldsymbol{s}dK - \int_K u\nabla\cdot\boldsymbol{s}dK + \int_{\partial K}\widehat{u}\boldsymbol{v}\cdot\boldsymbol{s}ds = 0. \tag{2.7f}$$

Summing up (2.7a)–(2.7f), we obtain

$$\begin{aligned}&\int_K u_t u dK + \int_K H^2 dK + \int_K \left(\frac{\boldsymbol{r}}{Q}\right)\cdot\boldsymbol{p}dK - \int_K (\boldsymbol{E}(\boldsymbol{r})\boldsymbol{p})\cdot\boldsymbol{r}dK\\ &\quad - \int_K \nabla\cdot(\boldsymbol{s}u) + \int_{\partial K}\widehat{\boldsymbol{s}\cdot\boldsymbol{v}}uds + \int_{\partial K}\widehat{u}\boldsymbol{v}\cdot\boldsymbol{s}ds\\ &\quad + \int_K \nabla\cdot(\boldsymbol{q}H)dK - \int_{\partial K}\widehat{\boldsymbol{q}\cdot\boldsymbol{v}}Hds - \int_{\partial K}\widehat{H}\boldsymbol{v}\cdot\boldsymbol{q}ds = 0.\end{aligned}$$

Using the relation

$$Q^2 = 1 + |\boldsymbol{r}|^2, \qquad \left(\frac{\boldsymbol{r}}{Q}\right)\cdot\boldsymbol{p} - (\boldsymbol{E}(\boldsymbol{r})\boldsymbol{p})\cdot\boldsymbol{r} = 0,$$

we have

$$\begin{aligned}&\int_K u_t u dK + \int_K H^2 dK - \int_K \nabla\cdot(\boldsymbol{s}u) + \int_{\partial K}\widehat{\boldsymbol{s}\cdot\boldsymbol{v}}uds + \int_{\partial K}\widehat{u}\boldsymbol{v}\cdot\boldsymbol{s}ds\\ &\quad + \int_K \nabla\cdot(\boldsymbol{q}H)dK - \int_{\partial K}\widehat{\boldsymbol{q}\cdot\boldsymbol{v}}Hds - \int_{\partial K}\widehat{H}\boldsymbol{v}\cdot\boldsymbol{q}ds = 0.\end{aligned}$$

Summing up over all elements K, with the numerical fluxes (2.5) and the periodic boundary conditions, we get

$$\int_\Omega u_t u d\Omega + \int_\Omega H^2 d\Omega = 0,$$

i.e.

$$\frac{1}{2}\frac{d}{dt}\int_\Omega u^2 d\Omega + \int_\Omega H^2 d\Omega = 0.$$

□

3 The LDG Method for the Willmore Flow of Graphs

In this section, we consider the local discontinuous Galerkin method for the Willmore flow of graphs equation (1.2) in $\Omega \in \mathbb{R}^d$ with $d \le 3$.

3.1 The LDG Method

In this section, we define our LDG method for the

To define the local discontinuous Galerkin method, we rewrite (1.2) as a first order system:

$$\frac{u_t}{Q} + \nabla \cdot (\boldsymbol{s} - \boldsymbol{v}) = 0, \tag{3.1a}$$

$$\boldsymbol{s} - \boldsymbol{E}(\boldsymbol{r})\boldsymbol{p} = 0, \tag{3.1b}$$

$$\boldsymbol{v} - \frac{1}{2}\frac{H^2}{Q}\boldsymbol{r} = 0, \tag{3.1c}$$

$$\boldsymbol{p} - \nabla W = 0, \tag{3.1d}$$

$$W - QH = 0, \tag{3.1e}$$

$$H - \nabla \cdot \boldsymbol{q} = 0, \tag{3.1f}$$

$$\boldsymbol{q} - \frac{\boldsymbol{r}}{Q} = 0, \tag{3.1g}$$

$$\boldsymbol{r} - \nabla u = 0, \tag{3.1h}$$

with

$$\boldsymbol{E}(\boldsymbol{r}) = \frac{1}{Q}\left(\boldsymbol{I} - \frac{\boldsymbol{r} \otimes \boldsymbol{r}}{Q^2}\right), \tag{3.2}$$

$$Q = \sqrt{1 + |\boldsymbol{r}|^2}, \tag{3.3}$$

where $\boldsymbol{s}$, $\boldsymbol{v}$, $\boldsymbol{p}$, $\boldsymbol{q}$, $\boldsymbol{r}$ are vectors, $\boldsymbol{E}(\boldsymbol{r})$ is the $d \times d$ matrix and $\boldsymbol{I}$ is the $d \times d$ identity matrix.

Applying the LDG method to the system (3.1), we have the scheme: Find u, H, $W \in V_h$, $\boldsymbol{s}$, $\boldsymbol{v}$, $\boldsymbol{p}$, $\boldsymbol{q}$, $\boldsymbol{r} \in \Sigma_h$, such that, for all test function φ, ξ, $\vartheta \in V_h$ and $\boldsymbol{\phi}$, $\boldsymbol{\psi}$, $\boldsymbol{\eta}$, $\boldsymbol{\rho}$, $\boldsymbol{\zeta} \in \Sigma_h$, we have

$$\int_K \frac{u_t}{Q}\varphi dK - \int_K (\boldsymbol{s} - \boldsymbol{v}) \cdot \nabla\varphi dK + \int_{\partial K} (\widehat{\boldsymbol{s} \cdot \boldsymbol{v}} - \widehat{\boldsymbol{v} \cdot \boldsymbol{v}})\varphi ds = 0, \tag{3.4a}$$

$$\int_K \boldsymbol{s} \cdot \boldsymbol{\phi} dK - \int_K \boldsymbol{E}(\boldsymbol{r})\boldsymbol{p} \cdot \boldsymbol{\phi} dK = 0, \tag{3.4b}$$

$$\int_K \boldsymbol{v} \cdot \boldsymbol{\psi} dK - \int_K \frac{1}{2}\frac{H^2}{Q}\boldsymbol{r} \cdot \boldsymbol{\psi} dK = 0, \tag{3.4c}$$

$$\int_K \boldsymbol{p} \cdot \boldsymbol{\eta} dK + \int_K W \nabla \cdot \boldsymbol{\eta} dK - \int_{\partial K} \widehat{W}\boldsymbol{v} \cdot \boldsymbol{\eta} ds = 0, \tag{3.4d}$$

$$\int_K W\xi dK - \int_K QH\xi dK = 0, \tag{3.4e}$$

$$\int_K H\vartheta dK + \int_K \boldsymbol{q} \cdot \nabla\vartheta dK - \int_{\partial K} \widehat{\boldsymbol{q} \cdot \boldsymbol{v}}\vartheta ds = 0, \tag{3.4f}$$

$$\int_K \boldsymbol{q} \cdot \boldsymbol{\rho} dK - \int_K \frac{\boldsymbol{r}}{Q} \cdot \boldsymbol{\rho} dK = 0, \tag{3.4g}$$

$$\int_K \boldsymbol{r}\cdot\boldsymbol{\zeta}dK + \int_K u\nabla\cdot\boldsymbol{\zeta}dK - \int_{\partial K}\widehat{u}\boldsymbol{v}\cdot\boldsymbol{\zeta}ds = 0, \tag{3.4h}$$

where $\boldsymbol{E}(\boldsymbol{r})$ and Q are computed by (3.2) and (3.3).

Similar to the development in [25], it turns out that we can take the simple choices for the numerical fluxes such that

$$\widehat{\boldsymbol{s}}|_e = \boldsymbol{s}_L, \qquad \widehat{\boldsymbol{v}}|_e = \boldsymbol{v}_L, \qquad \widehat{\boldsymbol{q}}|_e = \boldsymbol{q}_R, \qquad \widehat{W}|_e = W_L, \qquad \widehat{u}|_e = u_R. \tag{3.5}$$

3.2 Energy Stability

In this section, we prove the energy stability of the LDG method for the Willmore flow equation defined in the previous section.

Proposition 3.1 (Energy stability) *The solution of the Willmore flow equation using the schemes* (3.4)–(3.5) *satisfies energy stability*

$$\frac{1}{2}\frac{d}{dt}\int_\Omega H^2 Q d\Omega + \int_\Omega \frac{(u_t)^2}{Q}d\Omega = 0, \quad \forall u, H \in V_h. \tag{3.6}$$

Proof After taking the time derivative, we choose the test functions $\vartheta = W$, $\boldsymbol{\rho} = -\boldsymbol{p}$, $\boldsymbol{\zeta} = \boldsymbol{v} - \boldsymbol{s}$ in (3.4f), (3.4g) and (3.4h). Then we get

$$\int_K H_t W dK + \int_K \boldsymbol{q}_t\cdot\nabla W dK - \int_{\partial K}\widehat{\boldsymbol{q}_t\cdot\boldsymbol{v}}W ds = 0, \tag{3.7}$$

$$-\int_K \boldsymbol{q}_t\cdot\boldsymbol{p}dK + \int_K\left(\frac{\boldsymbol{r}}{Q}\right)_t\cdot\boldsymbol{p}dK = 0, \tag{3.8}$$

$$\int_K \boldsymbol{r}_t\cdot(\boldsymbol{v}-\boldsymbol{s})dK + \int_K u_t\nabla\cdot(\boldsymbol{v}-\boldsymbol{s})dK - \int_{\partial K}\widehat{u}_t\boldsymbol{v}\cdot(\boldsymbol{v}-\boldsymbol{s})ds = 0. \tag{3.9}$$

For (3.4a)–(3.4e), we take the test functions

$$\varphi = u_t, \qquad \boldsymbol{\phi} = \boldsymbol{r}_t, \qquad \boldsymbol{\psi} = -\boldsymbol{r}_t, \qquad \boldsymbol{\eta} = \boldsymbol{q}_t, \qquad \xi = -H_t.$$

Then we have

$$\int_K \frac{(u_t)^2}{Q}dK - \int_K(\boldsymbol{s}-\boldsymbol{v})\cdot\nabla u_t dK + \int_{\partial K}(\widehat{\boldsymbol{s}\cdot\boldsymbol{v}} - \widehat{\boldsymbol{v}\cdot\boldsymbol{v}})u_t ds = 0, \tag{3.10}$$

$$\int_K \boldsymbol{s}\cdot\boldsymbol{r}_t dK - \int_K \boldsymbol{E}(\boldsymbol{r})\boldsymbol{p}\cdot\boldsymbol{r}_t dK = 0, \tag{3.11}$$

$$-\int_K \boldsymbol{v}\cdot\boldsymbol{r}_t dK + \int_K \frac{1}{2}\frac{H^2}{Q}\boldsymbol{r}\cdot\boldsymbol{r}_t dK = 0, \tag{3.12}$$

$$\int_K \boldsymbol{p}\cdot\boldsymbol{q}_t dK + \int_K W\nabla\cdot\boldsymbol{q}_t dK - \int_{\partial K}\widehat{W}\boldsymbol{v}\cdot\boldsymbol{q}_t ds = 0, \tag{3.13}$$

$$-\int_K W H_t dK + \int_K Q H H_t dK = 0. \tag{3.14}$$

Summing up (3.7)–(3.14), we obtain

$$\begin{aligned}
&\int_K \frac{1}{2}\frac{H^2}{Q}\boldsymbol{r}\cdot\boldsymbol{r}_t dK + \int_K QHH_t dK + \int_K \frac{(u_t)^2}{Q}dK \\
&\quad + \int_K \left(\frac{\boldsymbol{r}}{Q}\right)_t \cdot \boldsymbol{p} dK - \int_K \boldsymbol{E}(\boldsymbol{r})\boldsymbol{p}\cdot\boldsymbol{r}_t dK \\
&\quad - \int_K \nabla\cdot((\boldsymbol{s}-\boldsymbol{v})u_t) + \int_{\partial K}(\widehat{\boldsymbol{s}\cdot\boldsymbol{v}} - \widehat{\boldsymbol{v}\cdot\boldsymbol{v}})u_t ds + \int_{\partial K}\widehat{u}_t\boldsymbol{v}\cdot(\boldsymbol{s}-\boldsymbol{v})ds \\
&\quad + \int_K \nabla\cdot(\boldsymbol{q}_t W)dK - \int_{\partial K}\widehat{\boldsymbol{q}_t\cdot\boldsymbol{v}}W ds - \int_{\partial K}\widehat{W}\boldsymbol{v}\cdot\boldsymbol{q}_t ds = 0.
\end{aligned}$$

Using the relation

$$Q_t = \frac{\boldsymbol{r}\cdot\boldsymbol{r}_t}{Q}, \qquad \left(\frac{\boldsymbol{r}}{Q}\right)_t = \boldsymbol{E}(\boldsymbol{r})\boldsymbol{r}_t,$$

we have

$$\begin{aligned}
&\int_K \frac{1}{2}H^2 Q_t dK + \int_K QHH_t dK + \int_K \frac{(u_t)^2}{Q}dK \\
&\quad - \int_K \nabla\cdot((\boldsymbol{s}-\boldsymbol{v})u_t) + \int_{\partial K}(\widehat{\boldsymbol{s}\cdot\boldsymbol{v}} - \widehat{\boldsymbol{v}\cdot\boldsymbol{v}})u_t ds + \int_{\partial K}\widehat{u}_t\boldsymbol{v}\cdot(\boldsymbol{s}-\boldsymbol{v})ds \\
&\quad + \int_K \nabla\cdot(\boldsymbol{q}_t W)dK - \int_{\partial K}\widehat{\boldsymbol{q}_t\cdot\boldsymbol{v}}W ds - \int_{\partial K}\widehat{W}\boldsymbol{v}\cdot\boldsymbol{q}_t ds = 0.
\end{aligned}$$

Summing up over K, with the numerical fluxes (3.5) and the periodic boundary conditions, we get

$$\int_\Omega \frac{1}{2}H^2 Q_t d\Omega + \int_\Omega QHH_t d\Omega + \int_\Omega \frac{(u_t)^2}{Q}d\Omega = 0,$$

i.e.

$$\frac{1}{2}\frac{d}{dt}\int_\Omega H^2 Q d\Omega + \int_\Omega \frac{(u_t)^2}{Q}d\Omega = 0. \qquad \square$$

4 Numerical Results

In this section we provide numerical examples to illustrate the accuracy and capability of the LDG method. Time discretization is by the forward Euler method with a suitably small Δt for stability. Since $\Delta t = O(h^4)$ due to the stability constraint, accuracy is maintained up to fourth order. This is not the most efficient method for the time discretization to our LDG scheme. However, we will not address the issue of time discretization efficiency in this paper. For all numerical simulations presented in this section, a domain with periodic boundary conditions is considered. We have verified with the aid of successive mesh refinements, that in all cases, the results shown are numerically convergent.

Table 1 Accuracy test for one-dimensional surface diffusion of graphs with exact solution (4.1). Uniform meshes with J cells at time $t = 0.5$

	J	L^∞ error	Order	L^2 error	Order
P^0	10	5.93E-03	–	1.37E-02	–
	20	2.95E-03	1.00	6.88E-03	0.99
	40	1.48E-03	1.00	3.45E-03	1.00
	80	7.38E-04	1.00	1.72E-03	1.00
P^1	10	8.00E-04	–	2.86E-03	–
	20	1.99E-04	2.00	7.17E-04	2.00
	40	4.98E-05	2.00	1.80E-04	1.99
	80	1.25E-05	2.00	4.51E-05	2.00
P^2	10	4.24E-05	–	1.76E-04	–
	20	5.29E-06	3.00	2.25E-05	2.96
	40	6.62E-07	3.00	2.83E-06	2.99
	80	8.75E-08	2.92	3.75E-07	2.92

4.1 Surface Diffusion of Graphs

In this section, we consider numerical simulations for surface diffusion of graphs equation (1.1).

Example 4.1 (Accuracy test) In this example, we consider the accuracy test for the one-dimensional surface diffusion of graphs. We test our method taking the exact solution

$$u(x,t) = 0.05\sin(x)\cos(t) \tag{4.1}$$

for the surface diffusion of graphs equation with a source term f, which is a given function so that (4.1) is the exact solution. The computational domain is $[-\pi,\pi]$. The L^2 and L^∞ errors and the numerical orders of accuracy at time $t = 0.5$ with uniform meshes are contained in Table 1. We can see that the method with P^k elements gives $(k+1)$-th order of accuracy in both L^2 and L^∞ norms.

Example 4.2 (Positive perturbation) We consider the numerical solutions of the two-dimensional surface diffusion of graphs equation (1.1) with the initial condition

$$u_0(x,y) = 1 + 0.3\min(1, \max(0, 2 - 5\sqrt{x^2+y^2})). \tag{4.2}$$

The computational domain is $[-1,1]$. We use P^2 elements with 40×40 uniform rectangular cells in our computation of the LDG method. The solutions at time $t = 0$, 0.0001, 0.001 and 0.005 are shown in Fig. 1. Even if we use a coarse mesh, we still obtain a good resolution of the solution comparable with that in [1]. We also observe similar phenomena as in [1]: a much faster smoothing effect for high frequencies than for low frequencies, as well as the solution becoming less than 1 (lack of maximum principle).

Example 4.3 (Perturbation with superposition of sines) We now consider numerical solutions of the two-dimensional surface diffusion of graphs equation (1.1) with the initial condition

$$u_0(x,y) = 1 + 0.1\sin(\pi(x+y)) + 0.3\sin(4\pi(x+y)). \tag{4.3}$$

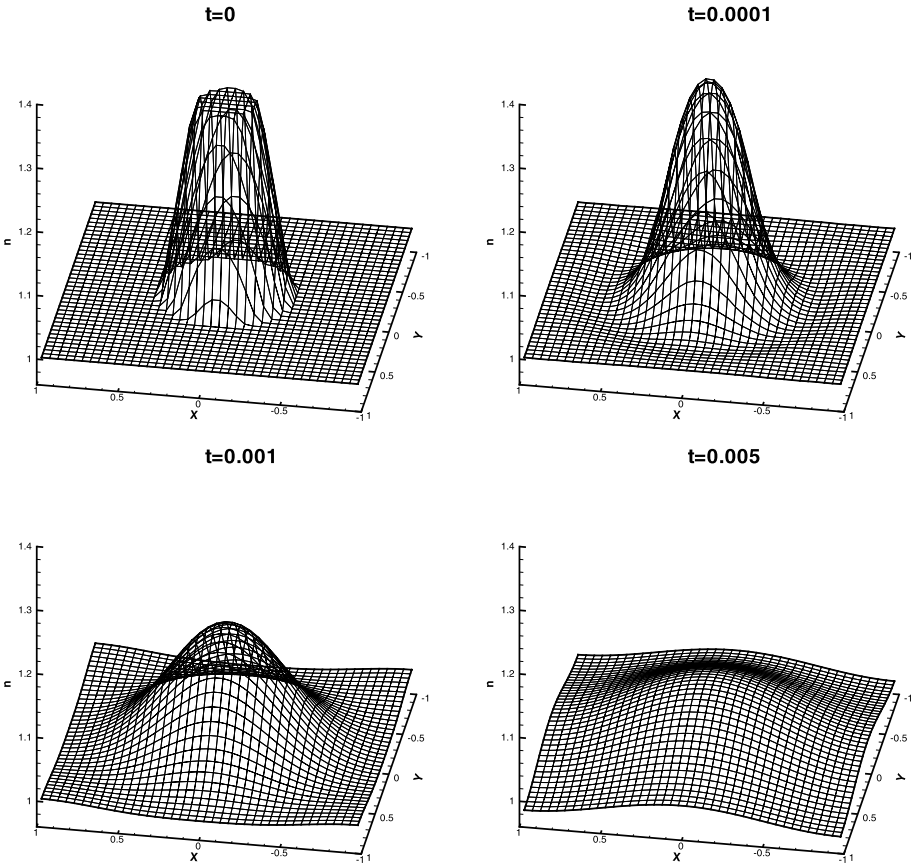

Fig. 1 The solution with positive perturbation of the surface diffusion of graphs equation (1.1) with the initial condition (4.2). Periodic boundary condition in $[-1, 1]$. P^2 elements and a uniform mesh with 40×40 cells

The computational domain is $[-1, 1]$. We use P^2 elements with 40×40 cells in our computation of the LDG method. The solutions at time $t = 0$, 0.0001, 0.001 and 0.00466 are shown in Fig. 2. There is a similar one-dimensional test case in [1]. The results show that high frequencies are rapidly damped and the amplitude of low frequency waves decays very slowly. The phenomenon is also similar to the one-dimensional test case in [1].

4.2 Willmore Flow of Graphs

In this section, we consider numerical simulations for the Willmore flow of graphs equation (1.2).

Example 4.4 (Accuracy test) We consider the accuracy test for one-dimensional Willmore flow of graphs. We test our method taking the exact solution

$$u(x, t) = 0.05 \sin(x) \cos(t) \tag{4.4}$$

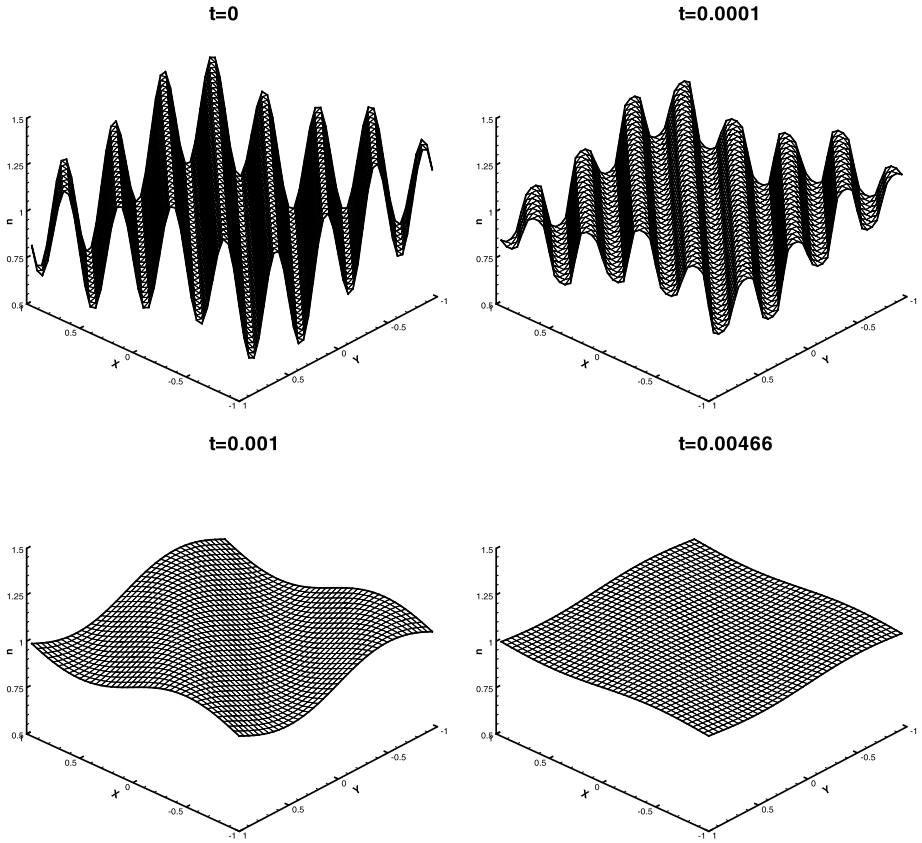

Fig. 2 The solution of the surface diffusion of graphs equation (1.1) with the initial condition (4.3). Periodic boundary condition in $[-1, 1]$. P^2 elements and a uniform mesh with 40×40 cells.

for the Willmore flow of graphs equation with a source term f chosen as a given function so that (4.4) is the exact solution. The L^2 and L^∞ errors and the numerical orders of accuracy at time $t = 0.5$ with uniform meshes are contained in Table 2. The computational domain is $[-\pi, \pi]$. We can see that the method with P^k elements gives $(k+1)$-th order of accuracy in both L^2 and L^∞ norms.

Example 4.5 (Convergence towards the planar surface) We consider the numerical solutions of the two-dimensional Willmore flow of graphs equation (1.2) with the initial condition

$$u_0(x, y) = \frac{1}{2} \sin\left(\pi \tanh\left(5(x^2 + y^2) - \frac{1}{4}\right)\right). \tag{4.5}$$

The computational domain is $[-2, 2]$. We use P^2 elements with 40×40 cells in our computation of the LDG method. The solutions at time $t = 0$, 0.001, 0.01 and 0.046 are shown in Fig. 3. A strong smoothing effect is much faster for high frequencies than for low frequencies. High frequencies are rapidly damped. The results are comparable with the results in [22].

Table 2 Accuracy test for one-dimensional surface diffusion of graphs with exact solution (4.1). Uniform meshes with J cells at time $t = 0.5$

	J	L^∞ error	Order	L^2 error	Order
P^0	10	1.17E-02	–	2.73E-02	–
	20	5.89E-03	0.99	1.37E-02	0.99
	40	2.95E-03	1.00	6.89E-03	1.00
	80	1.47E-03	1.00	3.45E-03	1.00
P^1	10	2.83E-03	–	1.03E-02	–
	20	7.23E-04	1.97	2.66E-03	1.96
	40	1.81E-04	2.00	6.70E-04	1.99
	80	4.41E-05	2.04	1.65E-04	2.02
P^2	10	4.74E-04	–	1.95E-03	–
	20	5.97E-05	2.99	2.51E-04	2.95
	40	7.83E-06	2.93	3.15E-05	3.00
	80	1.05E-06	2.90	4.07E-06	2.95

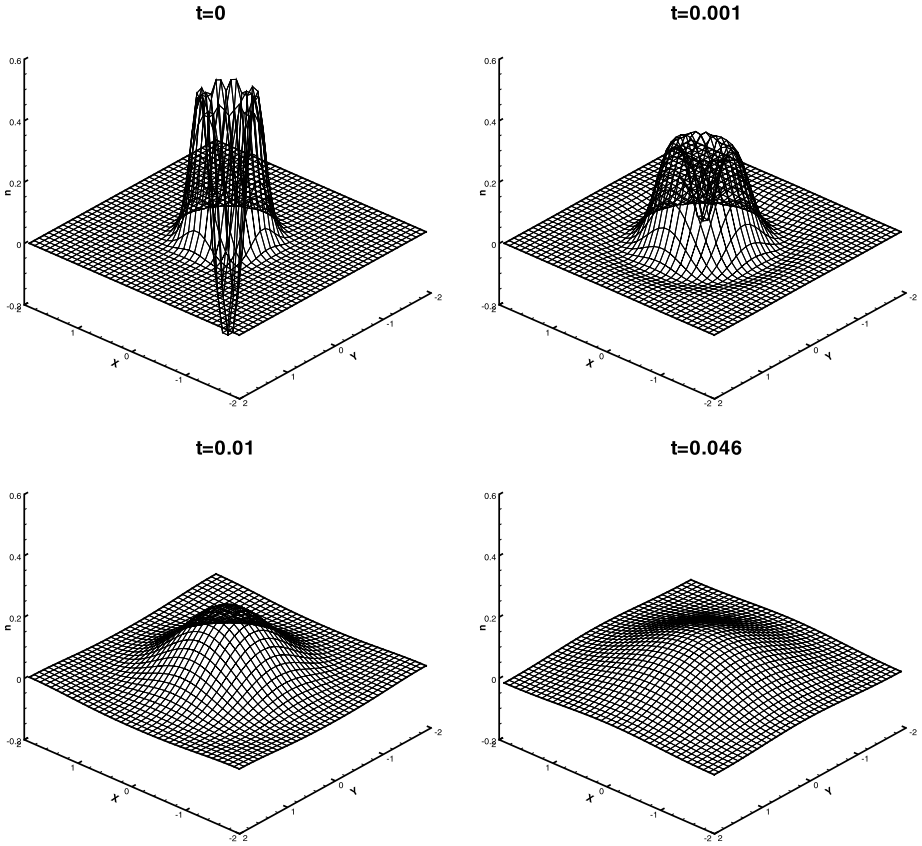

Fig. 3 The solution of the Willmore flow of graphs equation (1.2) with the initial condition (4.5). Periodic boundary condition in $[-2, 2]$. P^2 elements and a uniform mesh with 40×40 cells

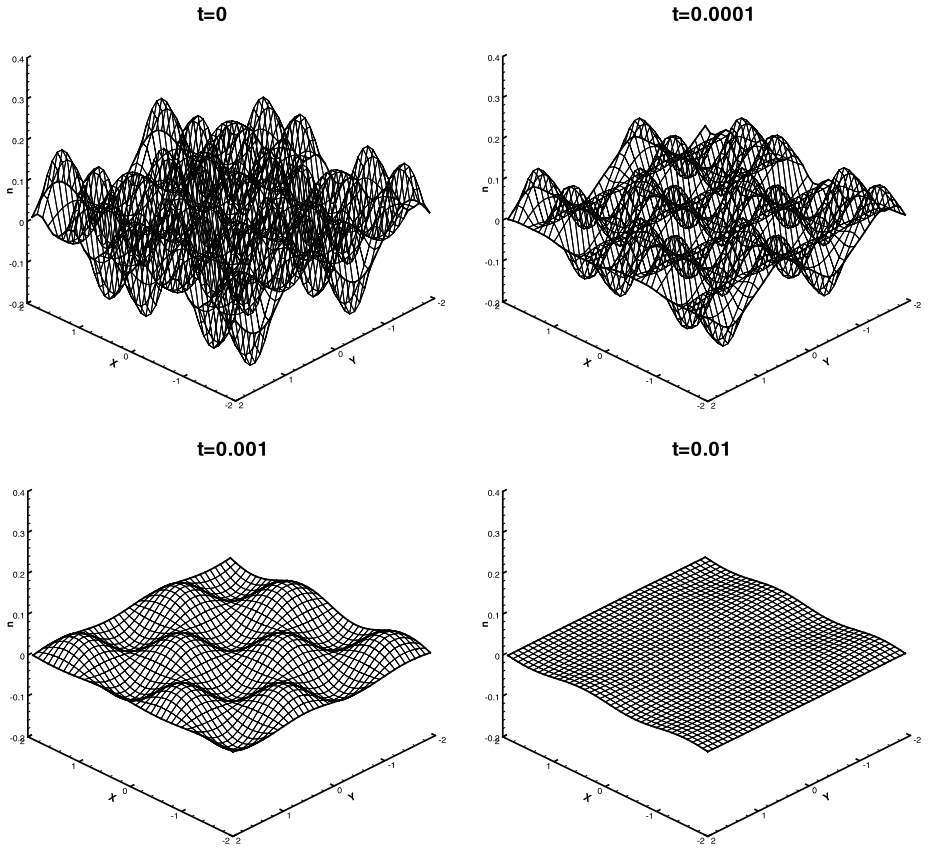

Fig. 4 The solution of the Willmore flow of graphs equation (1.2) with the initial condition (4.6). Periodic boundary condition in $[-2, 2]$. P^2 elements and a uniform mesh with 40×40 cells

Example 4.6 (Sine perturbation) We consider the numerical solutions of the two-dimensional Willmore flow of graphs equation (1.2) with the initial condition

$$u_0(x, y) = 0.25 \sin(\pi y)(0.25 \sin(\pi x) + 0.5 \sin(3\pi x)). \tag{4.6}$$

The computational domain is $[-2, 2]$. We use P^2 elements with 40×40 cells in our computation of the LDG method. The solutions at time $t = 0, 0.0001, 0.001$ and 0.01 are shown in Fig. 4. There is a similar numerical simulation in [14]. The results show that high frequencies are rapidly damped and the amplitude of the waves decays very fast as in [14].

5 Conclusion

We have developed a local discontinuous Galerkin method to solve the surface diffusion of graphs and Willmore flow of graphs equations. L^2 stability and energy stability are proven for general solutions. Numerical examples are given to illustrate the accuracy and capability

of the methods. Although not addressed in this paper, LDG methods are flexible for general geometry, unstructured meshes and h-p adaptivity. That will be our future work on solving nonlinear equations in geometric partial differential equations.

References

1. Bänsch, E., Morin, P., Nochetto, R.H.: Surface diffusion of graphs: variational formulation, error analysis, and simulation. SIAM J. Numer. Anal. **42**, 773–799 (2004)
2. Bassi, F., Rebay, S.: A high-order accurate discontinuous finite element method for the numerical solution of the compressible Navier-Stokes equations. J. Comput. Phys. **131**, 267–279 (1997)
3. Beneš, M.: Numerical solution for surface diffusion on graphs. In: Proceedings of Czech-Japanese Seminar in Applied Mathematics 2005, COE Lect. Note, 3, pp. 9–25. Kyushu Univ. The 21 Century COE Program, Fukuoka (2006)
4. Cockburn, B.: Discontinuous Galerkin methods for methods for convection-dominated problems. In: Barth, T.J., Deconinck, H. (eds.) High-Order Methods for Computational Physics. Lecture Notes in Computational Science and Engineering, vol. 9, pp. 69–224. Springer, Berlin (1999)
5. Cockburn, B., Shu, C.-W.: TVB Runge-Kutta local projection discontinuous Galerkin finite element method for conservation laws II: general framework. Math. Comput. **52**, 411–435 (1989)
6. Cockburn, B., Shu, C.-W.: The Runge-Kutta discontinuous Galerkin method for conservation laws V: multidimensional systems. J. Comput. Phys. **141**, 199–224 (1998)
7. Cockburn, B., Shu, C.-W.: The local discontinuous Galerkin method for time-dependent convection-diffusion systems. SIAM J. Numer. Anal. **35**, 2440–2463 (1998)
8. Cockburn, B., Shu, C.-W.: Runge-Kutta discontinuous Galerkin methods for convection-dominated problems. J. Sci. Comput. **16**, 173–261 (2001)
9. Cockburn, B., Shu, C.-W.: Foreword for the special issue on discontinuous Galerkin method. J. Sci. Comput. **22–23**, 1–3 (2005)
10. Cockburn, B., Lin, S.-Y., Shu, C.-W.: TVB Runge-Kutta local projection discontinuous Galerkin finite element method for conservation laws III: one dimensional systems. J. Comput. Phys. **84**, 90–113 (1989)
11. Cockburn, B., Hou, S., Shu, C.-W.: The Runge-Kutta local projection discontinuous Galerkin finite element method for conservation laws IV: the multidimensional case. Math. Comput. **54**, 545–581 (1990)
12. Coleman, B., Falk, R., Moakher, M.: Space-time finite element methods for surface diffusion with applications to the theory of the stability of cylinders. SIAM J. Sci. Comput. **17**, 1434–1448 (1996)
13. Dawson, C.: Foreword for the special issue on discontinuous Galerkin method. Comput. Methods Appl. Mech. Eng. **195**, 3183 (2006)
14. Deckelnick, K., Dziuk, G.: Error analysis of a finite element method for the Willmore flow of graphs. Interfaces Free Bound. **8**, 21–46 (2006)
15. Deckelnick, K., Dziuk, G., Elliott, C.M.: Computation of geometric partial differential equations and mean curvature flow. Acta Numer. **14**, 139–232 (2005)
16. Droske, M., Rumpf, M.: A level set formulation for Willmore flow. Interfaces Free Bound. **6**, 361–378 (2004)
17. Du, Q., Liu, C., Wang, X.: A phase field approach in the numerical study of the elastic bending energy for vesicle membranes. J. Comput. Phys. **198**, 450–468 (2004)
18. Du, Q., Liu, C., Ryham, R., Wang, X.: A phase field formulation of the Willmore problem. Nonlinearity **18**, 1249–1267 (2005)
19. Dziuk, G., Kuwert, E., Schätzle, R.: Evolution of elastic curves in $\mathbb{R}^n$: existence and computation. SIAM J. Math. Anal. **33**, 1228–1245 (2002)
20. Elliott, C.M., Maier-Paape, S.: Losing a graph with surface diffusion. Hokkaido Math. J. **30**, 297–305 (2001)
21. Escher, J., Mayer, U.F., Simonett, G.: The surface diffusion flow for immersed hypersurfaces. SIAM J. Math. Anal. **29**, 1419–1433 (1998)
22. Oberhuber, T.: Numerical solution for the Willmore flow of graphs. In: Proceedings of Czech-Japanese Seminar in Applied Mathematics 2005, COE Lect. Note, 3, pp. 126–138. Kyushu Univ. The 21 Century COE Program, Fukuoka (2006)
23. Reed, W.H., Hill, T.R.: Triangular mesh method for the neutron transport equation. Technical report LA-UR-73-479, Los Alamos Scientific Laboratory, Los Alamos, NM (1973)
24. Simonett, G.: The Willmore flow near spheres. Differ. Integral Equs. **14**, 1005–1014 (2001)
25. Xia, Y., Xu, Y., Shu, C.-W.: Local discontinuous Galerkin methods for the Cahn-Hilliard type equations. J. Comput. Phys. **227**, 472–491 (2007)

26. Xia, Y., Xu, Y., Shu, C.-W.: Application of the local discontinuous Galerkin method for the Allen-Cahn/Cahn-Hilliard system. Commun. Comput. Phys. **5**, 821–835 (2009)
27. Xu, Y., Shu, C.-W.: Local discontinuous Galerkin methods for nonlinear Schrödinger equations. J. Comput. Phys. **205**, 72–97 (2005)
28. Xu, Y., Shu, C.-W.: Local discontinuous Galerkin methods for two classes of two dimensional nonlinear wave equations. Physica D **208**, 21–58 (2005)
29. Yan, J., Shu, C.-W.: A local discontinuous Galerkin method for KdV type equations. SIAM J. Numer. Anal. **40**, 769–791 (2002)